ACS Sustainable Chemistry & Engineering

pubs.acs.org/journal/ascecg

Research Article

Potential To Produce Sugars and Lignin-Containing Cellulose Nanofibrils from Enzymatically Hydrolyzed Chemi-Thermomechanical Pulps

Xushen Han, Ran Bi, Hale Oguzlu, Masatsugu Takada, Jungang Jiang, Feng Jiang,* Jie Bao, and Jack N. Saddler*

Cite This: *ACS Sustainable Chem. Eng.* 2020, 8, 14955−14963

Read Online

ACCESS | Metrics & More | Article Recommendations | Supporting Information

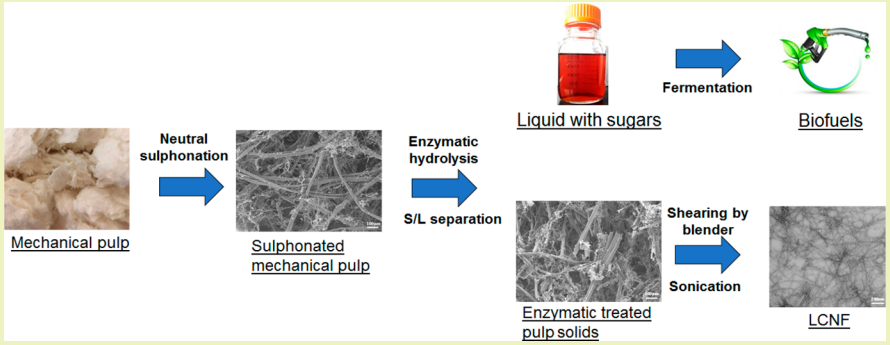

ABSTRACT: Softwood mechanical pulps have proven to be quite recalcitrant to enzymatic hydrolysis. However, the unhydrolyzed, residual fibers might have potential as nanofibrillated cellulose feedstocks. In the work reported here, a bleached softwood chemi-thermomechanical pulp (CTMP) was neutrally sulfonated (S-BCTMP) in an attempt to enhance fiber accessibility and enzymatic hydrolysis. A 12 h hydrolysis at 10% solid loading with CTec3 cellulases provided optimum conditions with 22% of the pulp hydrolyzed to monosaccharides and about one-third of the original substrate remaining as lignin-containing cellulose nanofibrils (LCNFs). Prolonged hydrolysis (72 h) resulted in 42% hydrolysis of the original substrate with only 16% of the original S-BCTMP recovered as LCNFs. Although the LCNFs contained high levels of lignin (26.8%−38.5%), they were successfully used to prepare transparent films showing a high contact angle (82.8°) and strong UV-blocking properties. It was apparent that enzyme-mediated modification of CTMP has the potential to produce both fermentable sugars and higher-value LCNFs.

KEYWORDS: *Lignin-containing cellulose nanofibrils (LCNFs), Chemi-thermomechanical pulp (CTMP), Neutral sulphonation, Enzymatic treatment, Cellulase cocktails*

INTRODUCTION

Nanocellulosic materials such as cellulose nanofibrils (CNFs) have shown considerable potential in various value-added areas such as nanocomposites, packaging, films, and paperboard applications.[1−4] Several nanocellulosic materials are produced by mechanical methods such as refining, grinding, ultrasonication, and homogenization (using homogenizers and microfluidizers).[5] However, to try to reduce the high energy input of mechanical treatments and to improve the homogeneity of the CNFs, various chemical/biological treatments have also been assessed for their potential to open up the structure of the lignocellulosic materials prior to mechanical treatment. To date, most chemical processes (2,2,6,6-tetramethylpiperidine-1-oxyl (TEMPO) oxidation, carboxymethylation, sulphonation, and cationization) have proven to be relatively expensive and typically come with considerable environmental concerns.[5−8] More recently, biological processes such as enzymatic treatments have attracted increased attention due to their potential to facilitate nanofibrillation under more environmentally friendly reaction conditions.[9−11] The most established feedstocks that have been used to make CNFs are bleached chemical pulps (Kraft or sulfite pulps),[1,5] with only a few studies assessing the potential of lignin-containing, high-yield pulps to make CNFs via chemical/biological treatments.[12−15]

High-yield pulps, such as thermomechanical pulp (TMP), chemi-thermomechanical pulp (CTMP), and bleached chemi-

Received: July 14, 2020
Revised: September 3, 2020
Published: September 17, 2020

https://dx.doi.org/10.1021/acssuschemeng.0c05183
ACS Sustainable Chem. Eng. 2020, 8, 14955−14963

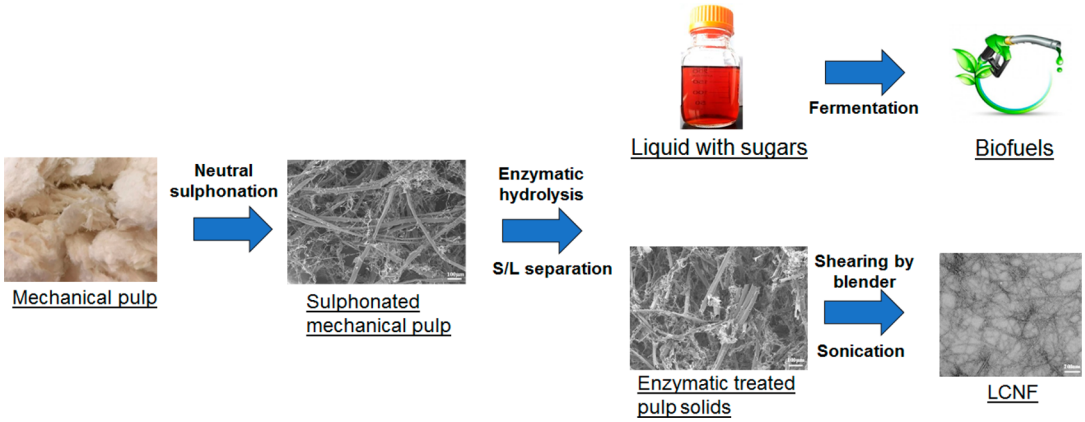

Figure 1. Diagram of the integrated production of LCNFs and sugars.

thermomechanical pulp (BCTMP), typically have the advantage of lower cost, less biomass loss, and reduced environmental pollution when compared to chemical pulps.[16,17] Although TMP, CTMP, and BCTMP continue to be major products derived from Canadian softwoods, their market demand has been in steep decline, primarily due to the digitalization of newspapers. Consequently, there is considerable interest in expanding the product portfolio that can be derived from mechanical pulps.

One approach that has been proposed is to repurpose TMP mills as the pretreatment "front end" of a bioconversion process for enzyme-mediated hydrolysis of pulps to fermentable sugars. However, high enzyme loadings are typically required, and the recalcitrance of softwoods to hydrolysis has proven to be challenging.[18] As discussed in more detail here, an alternative approach could be to produce both sugars and higher-value nanofibrils from the unhydrolyzed residues. It is likely that nanofibrils derived from mechanical pulps will contain hemicellulose and lignin, which should endow them with several interesting characteristics and differentiate them from traditional nanofibrils derived from chemical pulps. For example, the hemicellulose in nanofibrils should help improve the aqueous stability of fibrils and prevent coalescence.[19] In parallel, much of the lignin component will be located on the surface of the nanofibrils, introducing amphiphilicity and likely improving its compatibility with hydrophobic oils or polymers.[12,20−22] Because lignin-containing cellulose nanofibrils (LCNFs) will have less polarity and higher hydrophobicity, this should also significantly increase the mechanical, thermal, and water barrier properties of any resulting composite,[6,23−25] with smoother surfaces and less micropores in the nanofibrils.[26]

However, past work has shown that, during the production of LCNFs from mechanical pulps, the lignin component restricts chemical and enzyme access to the cellulose, preventing the nanofibrillation of the cellulose.[23,27] Similarly, although hemicellulose has been shown to restrict microfibril coalescence and facilitate pulp nanofibrillation,[28] it is anticipated that the relatively intact lignocellulosic matrix of mechanical pulps will restrict effective nanofibrillation. For example, effective production of LCNFs from mechanical pulp via mechanical grinding, disk refining, and homogenization can only be achieved at the expense of high energy costs.[12,14,29] Similarly, possible chemical treatments such as TEMPO oxidation have been shown to facilitate mechanical pulp nanofibrillation but again with the need for expensive oxidants, which further increases costs.[15,30]

In the work reported here, a softwood BCTMP was neutrally sulfonated in an attempt to increase its accessibility to cellulase enzymes, consequently enhancing both fibrillation and hydrolysis. At various times during hydrolysis, the insoluble fibers were withdrawn and further disintegrated via blending and ultrasonication to produce LCNFs. The chemical, morphological, and thermal properties of the LCNFs were assessed using X-ray diffraction (XRD), Fourier transform infrared spectroscopy (FTIR), scanning electron microscopy (SEM), transmission electron microscopy (TEM), atomic force microscopy (AFM), and thermogravimetric analysis (TGA). As reported here, effective pretreatment of the BCTMP resulted in enhanced cellulose hydrolysis while producing LCNFs with potential applications in the evolving biomaterial markets.

EXPERIMENTAL SECTION

Pulp and Chemicals. Bleached softwood chemi-thermomechanical pulp (BCTMP) composed of spruce, pine, and fir was provided by Quesnel River Pulp, Ltd., Canada. The BCTMP was washed 10 times (w/w) with deionized water and then disintegrated. It was consequently vacuum-filtrated to a moisture content of 80% and stored at 4 °C before use. Other reagents were analytical-grade and provided by Fisher Scientific, U.S.A.

Neutral Sulphonation Treatment of BCTMP. The disintegrated BCTMP was subjected to neutral sulphonation according to the procedures of Chandra et al.[31] Briefly, sulphonation was conducted in a Parr high-pressure batch reactor (1 L capacity, T 316 stainless steel, Parr Instrument Company, Moline, IL) at a 10% (w/w) consistency with a Na_2SO_3 dosage of 0.16 g/g of dry pulp at 160 °C for 1 h. The treated slurry was then washed using deionized water and filtrated until the conductivity of the liquid fraction was <5 μS/cm. The wet solids fraction (80% moisture content) was stored at 4 °C before use.

Enzymatic Treatment and Mechanical Treatment. The sulfonated BCTMP (S-BCTMP) was suspended in acetate buffer (50 mM, pH 5.0) at 50 °C for 2 h and then hydrolyzed using the cellulase cocktail Cellic CTec 3 (Novozymes, Bagsvaerd, Denmark) at a dosage of 20 mg of protein/g of cellulose at 50 °C and 180 rpm. The solids loading was 10% (w/w). The hydrolysis yield of glucan, xylan, mannan, arabinan, and galactan was calculated based on the corresponding polysaccharide weight. After a specific hydrolysis time, enzymatic hydrolysis was terminated by heating the mixture at 85 °C for 20 min. The solid residue was then washed and filtered until the conductivity of the liquid fraction approached that of deionized water.

The water-insoluble fraction of hydrolyzed S-BCTMP was prepared in a suspension at 0.25% (w/w) consistency and

https://dx.doi.org/10.1021/acssuschemeng.0c05183
ACS Sustainable Chem. Eng. 2020, 8, 14955−14963

Table 1. Chemical Composition of BCTMP and Sulfonated BCTMP

	Klason lignin (%)	glucan (%)	xylan (%)	arabinan (%)	galactan (%)	mannan (%)
BCTMP	24.6 ± 1.4	44.0 ± 1.1	5.4 ± 0.3	1.3 ± 0.1	2.0 ± 0.1	9.5 ± 0.6
S-BCTMP	20.1 ± 0.9	48.9 ± 0.9	5.3 ± 0.4	1.0 ± 0.1	1.7 ± 0.2	8.9 ± 0.5

mechanically sheared (~20 000 rpm) using a household blender (Vitamix 6300, U.S.A.) for 30 min, followed by ultrasonication (Fisher Model 700) at a 90% amplitude for 30 min. The slurry was centrifuged at 5 000 rpm for 30 min. The supernatant was defined as the LCNF aqueous suspension. The concentration/weight of LCNFs was determined by oven-drying 10 mL of the suspension at 105 °C. Distilled water was used as a blank.[32,33] The yield of LCNFs was calculated as follows:

$$\frac{(\text{concentration of LCNFs} \times \text{volume of LCNF suspension})}{\text{mass of S-BCTMP before enzymatic hydrolysis}} \quad (1)$$

The overall integrated production of LCNFs and sugars is summarized in Figure 1.

Preparation of Lignin-Containing Cellulose Nanofibril Film. The LCNF suspension was concentrated to a 0.1% solids content by vacuum-rotary evaporation at 50 °C. Then 40 mL of the lignin-containing cellulose nanofibril (LCNF) suspension was poured slowly onto a 0.22 μm nylon membrane (diameter 47 mm) followed by vacuum-filtration until a dried thin film was formed. The dried film was peeled off and stored in a conditioned room with 50% relative humidity at 23 °C before testing.

Characterization. *Compositional Analysis.* The chemical composition of the substrates was determined according to TAPPI Standard Method T-222. The sugar content was measured by a Dionex DX-3000 HPLC (Sunnyvale, CA) equipped with an anion-exchange column (Dionex CarboPac PA1), and the Klason lignin content was measured as the residual mass after filtration through a G3 sintered glass funnel.[32,34]

Cellulase Accessibility and Enzymatic Hydrolysis. The water retention value (WRV) was determined and calculated according to TAPPI Useful Method-256. The WRV is the percentage of the retained water based on the dried substrate after centrifugation at 900 × *g* for 30 min. Direct Orange staining was performed to assess the changes in specific surface area according to the modified Simons' stain method.[35] The acid groups in the pretreated substrates were determined by the conductometric titration method as described by Katz et al.[36] The width and length of the fibers were determined using a fiber quality analyzer (FQA, LDA02; OpTest Equipment, Inc., Hawkesbury, ON, Canada) according to the procedure described previously.[34]

The enzymatic hydrolysis assay was performed in acetate buffer (50 mM, pH 5.0) at 2% consistency (w/v), 30 mg of CTec 3 enzymes protein per gram of cellulose, 50 °C, and 150 rpm for 72 h to assess enzyme-accessibility improvements to BCTMP after sulphonation treatment. After hydrolysis, the sugar content was assayed by high-performance liquid chromatography (HPLC) and cellulose hydrolysis yield was calculated accordingly.[31] Experiments were performed in triplicate, and the values shown were the average of the three measurements.

Transmission Electron Microscopy. Formvar coated carbon grids (300 mesh copper, Ted Pella, Inc., Redding, CA) were used as substrates for transmission electron microscopy (TEM) imaging. Prior to sample preparation, the grids were glow-discharged for 10 s to enhance their hydrophilicity. The LCNF suspension (0.01 wt %, 8 μL) was deposited on the grids, and the excess liquid was removed by blotting with filter paper. The grids were then negatively stained with 2% uranyl acetate solution and dried under ambient conditions. The samples were observed using a Hitachi H7600 transmission electron microscope operated at a 100 kV accelerating voltage. The widths of the LCNFs from the TEM images were quantified using the software ImageJ from over 100 individual LCNFs.

Atomic Force Microscopy. The morphologies of the LCNFs were also observed using atomic force microscopy (Bruker, Inc., U.S.A., MultiMode 8) equipped with a J scanner. A droplet of 0.001 wt % LCNF suspension was deposited onto a freshly cleaved mica disc with a diameter of 12 mm and dried at room temperature. Height profiles were obtained with an aluminum-coated antimony-doped silicon cantilever (spring constant 40 N/m, resonance frequency ca. 300 kHz, VTESPA-300, Bruker, Inc.) in peak force tapping mode.

Scanning Electron Microscopy. Lignin-containing cellulose nanofibril (LCNF) (0.1 wt %) suspensions were frozen in liquid nitrogen and then freeze-dried (Labconco, U.S.A.) for characterization. The morphologies of the freeze-dried materials (pulp, enzymatic hydrolyzed pulp, and LCNFs) were characterized using a scanning electron microscope (Hitachi S4700) at a working distance of 5 mm and an accelerating voltage of 5 kV. All samples were sputter-coated with 9 nm of gold using a Cressington high-resolution sputter coater (Ted Pella, Inc., Sweden) prior to imaging.

UV−Vis Spectroscopy. The light transmittance of the LCNF suspension (0.1 wt %, w/v) and the light absorbance of the LCNF suspension (0.01 wt %, w/v) were measured from 200 to 800 nm wavelength using a Cary 50 UV−vis spectrophotometer.

Zeta Potential. The zeta potential was measured using a Zetasizer nano-ZS (Malvern, CA) at 0.1 wt %.

ATR-FTIR Spectra Analysis. FTIR spectra of freeze-dried pulp and LCNFs were assayed by an FTIR spectrometer (PerkinElmer, Wellesley, MA) with a universal attenuated total reflectance (ATR) accessory from 500 to 4000 cm^{-1} and a resolution of 4 cm^{-1}, with a total of 80 scans.

X-ray Diffraction Analysis. X-ray diffraction patterns (XRD) of freeze-dried pulp and LCNFs were collected on a Bruker D8-Advance powder X-ray diffractometer, using Cu Ka radiation (k = 0.1540 nm) generated at 40 kV and 40 mA. All scans were obtained from 5 to 80° (2θ) with a step interval of 0.04°.

The peaks were deconvoluted using PeakFit (www.systatsoftware.com) by assuming Gaussian functions for each peak, and a broad peak centered at 20° was assigned as an amorphous peak. Iterations were repeated until the maximum F number reached over 10 000 with an R^2 value above 0.997. The crystallinity index (CrI) was calculated as the percentage of the area of all crystalline peaks over the total area.[37]

The average crystallite dimension L was calculated using the Scherrer equation.[38]

$$L = \frac{0.9\lambda}{\beta_{1/2}\cos\theta} \quad (2)$$

where λ is the X-ray radiation wavelength (1.54 Å), $\beta_{1/2}$ is the full width at half-maximum of the diffraction peak, and θ is the corresponding Bragg angle.

Thermogravimetric Analysis. Thermogravimetric analysis (TGA) of the freeze-dried samples was carried out using a thermogravimetric analyzer (NETZSCH, TG 209F1, Germany). Approximately 10 mg of each sample was heated from room temperature to 600 °C with a heating rate of 20 °C/min under a 20 mL/min nitrogen stream.

Contact Angle. The water contact angle of the LCNF film was measured with a DataPhysics PSL 250 contact angle analyzer (Future Digital Scientific Corp., GmbH, Germany). 4 μL of deionized water was dropped onto the LCNF film using a microsyringe. The contact angle was measured every 30 s for 2 min. Experiments were performed in triplicate, and the data shown here were taken from the average of the three measurements.

UV-Blocking Test. The UV-blocking performance of the LCNF film was demonstrated by illuminating a UV pattern using a UV flashlight at a distance of 50 cm. The LCNF film was placed between

https://dx.doi.org/10.1021/acssuschemeng.0c05183
ACS Sustainable Chem. Eng. 2020, 8, 14955−14963

Table 2. Cellulase Accessibility of BCTMP and Sulfonated BCTMP

	acid groups (mmol/kg)				direct orange dye	
	strong	weak	added sulfonic group	water retention value (%)	adsorption (mg/g)	enzymatic cellulose conversion yield (%)
BCTMP	55 ± 5	262 ± 9	ND	209 ± 14	44 ± 5	27.9 ± 2.1
S-BCTMP	148 ± 6	212 ± 8	93 ± 6	257 ± 21	60 ± 6	72.1 ± 3.4

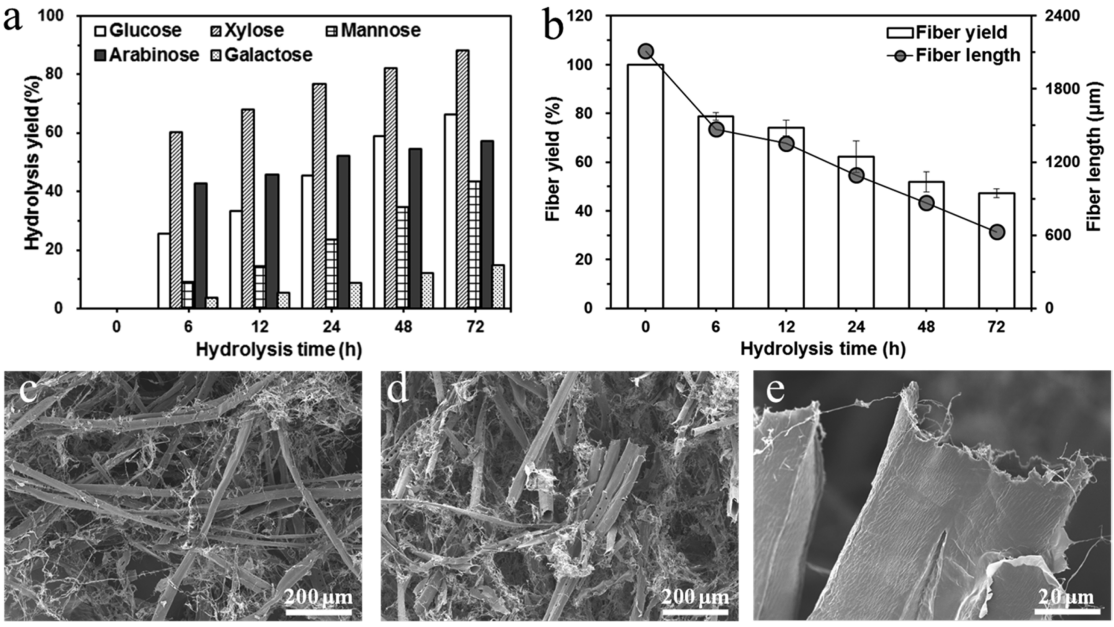

Figure 2. Enzymatic hydrolysis of sulfonated BCTMP. (a) Hydrolysis yield; (b) fiber yield and length; (c) SEM image of S-BCTMP; (d, e) SEM images of S-BCTMP-H12.

the UV source and the pattern to observe the blocking effects with a polyethylene (PE) film of similar thickness used as a control.

RESULTS AND DISCUSSION

Increasing Cellulase Enzyme Accessibility to Bleached Softwood Chemi-thermomechanical Pulps by Neutral Sulphonation. Typically, the combination of chemi-thermomechanical pulping and bleaching (BCTM) results in high-yield pulps (usually >90%) that require minimum chemical and refining energy inputs. As anticipated, the BCTM pulp contained ~25% lignin (Table 1), close to the lignin content of the original softwood chips,[16,17] because the relatively mild treatments are primarily used to soften the lignin and reduce refining energy inputs. Related work has also shown that bleaching CTM pulps does not remove lignin but rather modifies the chromophores to reduce the color intensity.[16,17] During the BCTMP pulping process, although the lignin in the middle lamella is disrupted, most of the cell wall structure remains intact.[17] This results in both high yields and good mechanical properties for applications such as newsprint. However, compared to hardwood mechanical pulps, the more condensed nature of softwood lignins, as a result of its higher guaiacyl content, restricts its hydrolysis and nanofibrillation.[9,39] As observed previously,[40] and as indicated in Table 2, even after 72 h of hydrolysis at a high enzyme loading (30 mg/g of cellulose), the cellulose within the BCTMP was poorly hydrolyzed (27.9%).

Because past work had shown that neutral sulphonation of wood chips enhanced cellulose accessibility and hydrolysis,[31,39] a similar strategy was followed to see if this could be repeated. It was apparent that, although the lignin decreased slightly from 24.6% to 20.1% and the cellulose increased from 44.0% to 48.9%, the hemicellulose content remained largely unchanged (Table 1). It was also apparent that, although the fiber length and width remained essentially the same before and after sulphonation, the sulfonic group content, WRV, and direct orange dye adsorption all increased (Table 2) due to the introduction of hydrophilic sulfonic acid groups resulting in increased fiber swelling.[39] Earlier work has also shown that sulphonation of the lignin present in wood chips makes the lignin more hydrophilic and inhibits the hydrophobic interactions between cellulase and lignin.[31] Thus, as a result of both decreased nonproductive binding of the enzymes to the lignin and increased enzyme accessibility, cellulose hydrolysis yield increased significantly from 27.9% to 72.1% (Table 2).

Possible Integrated Sugars and LCNFs Production Using Limited Enzymatic Hydrolysis. Enzyme-mediated cellulose hydrolysis has typically been carried out at relatively low substrate concentrations, using high enzyme loadings, over prolonged (72 h) periods of time,[41] with incomplete hydrolysis of the substrate often occurring even after extended incubation times. Thus, while sulphonation has been shown to increase initial hydrolysis, it is possible that the more recalcitrant, residual fibers might prove to be a potential source of nanofibrillated material. Past work has shown that cellulases could hydrolyze chemical pulps into fermentable sugars while producing potential nanocellulosic feedstocks.[11,42] Although BCTM pulps can be hydrolyzed to sugar feedstocks for biofuels and biobased chemicals production,[43] the concentration needs to be as high as possible to avoid costly concentration processes and satisfy the requirements of

https://dx.doi.org/10.1021/acssuschemeng.0c05183
ACS Sustainable Chem. Eng. 2020, 8, 14955−14963

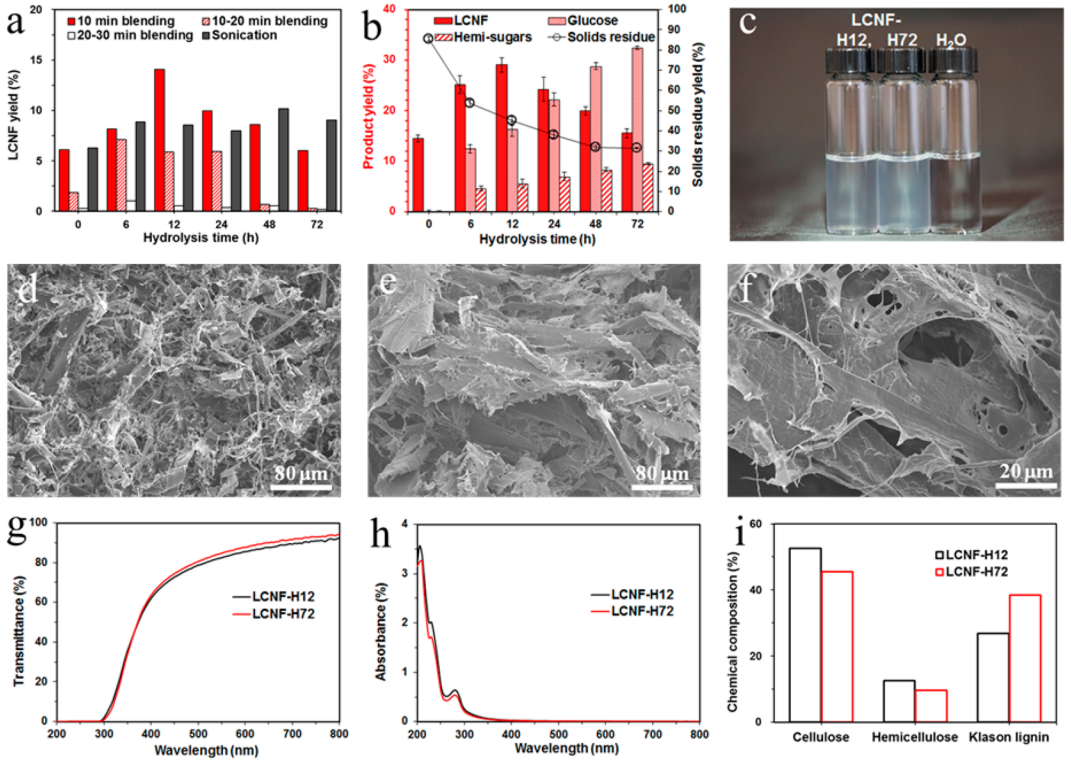

Figure 3. LCNF yield and suspension characterization. (a) LCNF yield; (b) overall yield of LCNFs, sugars, and solid residues; (c) photos of LCNF suspensions in comparison with water; (d) SEM image of S-BCTMP-H12-B30; (e, f) SEM images of S-BCTMP-H12-B30-S30; (g) UV−vis transmittance of 0.1 wt % LCNF suspensions; (h) UV−vis absorbance of 0.01 wt % LCNF suspensions; (i) chemical composition of LCNFs. S-BCTMP-H12-B30 is S-BCTMP after 12 h of enzymatic treatment and 30 min of blending; S-BCTMP-H12-B30-S30 is S-BCTMP after 12 h of enzymatic treatment, 30 min of blending, and 30 min of sonication.

industrial fermentations.[44−47] Related work has shown that, if pulp concentrations are >10%, insufficient mixing typically occurs, severely limiting hydrolysis.[41]

It was apparent that increasing the hydrolysis time from 6 to 72 h increased both the hydrolysis yield and sugar concentrations (Figure 2a). However, after the relatively rapid (12 h) hydrolysis of the sulfonated BCTMP (S-BCTMP), further hydrolysis occurred much more slowly with the fiber yield and length continuing to decrease as the hydrolysis proceeded (Figure 2b). Although the S-BCTMP fibers were initially long and fibrillated, likely due to mechanical refining (Figure 2c), after 12 h of hydrolysis, the fibers were shorter with broken ends (Figure 2d). The much shorter, broken fibers that were observed were in agreement with the reduced fiber lengths determined by fiber quality analysis (FQA) (Figure 2b). The higher-magnification images of the broken ends, which showed uneven cross-sectional surfaces and some ruptures along the longitudinal directions, were likely due to enzymatic action (Figure 2e). Previous work has suggested that these shorter and degraded fibers are a result of the more rapid hydrolysis of the less-organized regions of the fibers by endoglucanase.[48−50] Because lignin significantly contributes to biomass recalcitrance, we next wanted to assess whether a combination of neutral sulphonation and enzymatic treatment could facilitate both cellulose hydrolysis and the nanofibrillation of the unhydrolyzed, residual material.

As mechanical blending is a low-power defibrillation treatment that has been successfully used to defibrillate cellulose nanofibrils after chemical modification,[51,52] we next assessed whether the residual, insoluble fibers could be defibrillated using a household blender (~20 000 rpm, 30 min) followed by ultrasonication (90% amplitude, 30 min) to produce lignin-containing cellulose nanofibrils (LCNFs). After 30 min of blending, ~8.2% of the original S-BCTMP could be converted to LCNFs (Figure 3a), similar to the 12% CNFs produced previously from rice straw.[52] However, the production of LCNFs could be increased by incorporating enzyme treatments, with a maximum obtained (20.5%) after 12 h of hydrolysis. Additional ultrasonication treatment increased the LCNF yields by ~6%−10%, with the overall LCNF yields obtained after hydrolysis, mechanical defibrillation, and ultrasonication all being higher than that of S-BCTMP without enzymatic hydrolysis. The highest LCNF yields (29.0%) were obtained after 12 h of hydrolysis, with prolonged hydrolysis resulting in the production of more sugars and less LCNFs (Figure 3b).

It should be noted that the relatively low yields obtained were probably a result of the limited energy input and restricted mechanical shearing forces resulting from the use of a household blender and ultrasonication. After 30 min of blending, the residual fibers appeared shorter, delaminated, and fibrillated (Figure 3d), while additional ultrasonication resulted in a decrease in fiber structure, leading to flattened and more nanofibrillated structures containing internal pores (Figure 3e and f). This suggested that, although ultrasonication resulted in an increase in accessibility to the hydrolyzed S-BCTMP, it did not lead to enhanced defibrillation due to the higher lignin content of the residual fibers.

Characterization of the LCNFs after Enzyme Treatment of Sulfonated Mechanical Pulps. *Stability and Characterization of LCNF Suspensions.* Aqueous suspensions of both LCNF-H12 and LCNF-H72 were clear and trans-

https://dx.doi.org/10.1021/acssuschemeng.0c05183
ACS Sustainable Chem. Eng. 2020, 8, 14955−14963

parent (Figure 3c) with the respective zeta potential values of −32.7 and −36.1 mV, indicating good stability. Previous work has shown that a zeta potential lower than −30 mV can help stabilize colloidal nanoparticle suspensions.[53] Both LCNF-H12 and LCNF-H72 suspensions showed high transmittance (92.4% and 94.5%) at 800 nm, indicating that, at the nanoscale, both of the LCNFs did not scatter visible light (Figure 3g). Zero transmittance values were observed for both of the LCNF suspensions at a 300 nm wavelength, indicating strong absorbance, while the absorbance peaks at 230 and 280 nm could be ascribed to the aromatic chromophores of softwood lignin structures (Figure 3h).[54−56] Although the two LCNFs had a similar chemical composition (Table S1), more lignin was present in LCNF-H72 due to the greater hydrolysis of the original substrate.

LCNF Morphologies. As the LCNFs obtained after blending and ultrasonication showed similar nanofibril-like structures with well-dispersed nanofibril-like morphologies (Figure S1), they were combined for subsequent characterization and use. The average widths of LCNF-H12 and LCNF-H72 were 7.6 and 7.1 nm, respectively (Figure S2). The LCNF-H72 sample also contained several dark spherical particles, ranging from 50 to 200 nm, likely indicating the presence of lignin nanoparticles (Figure 4a and b). Similar lignin nanoparticles have

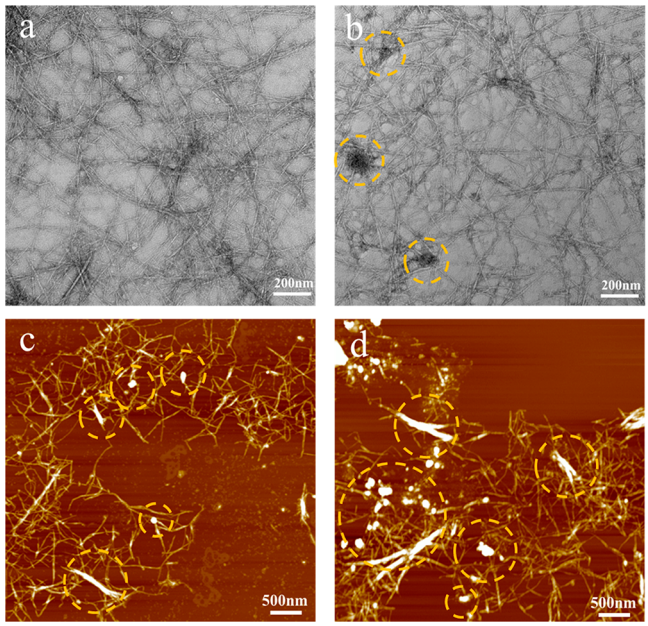

Figure 4. Microscopy images of LCNFs. (a, b) TEM and (c, d) AFM images of LCNF-H12 and LCNF-H72, respectively.

been previously observed in LCNFs prepared by mechanical grinding,[20] with the lignin tending to aggregate into spherical nanoparticles due to its aromatic structure and amphiphilic nature.

When the LCNFs and lignin aggregates were investigated using AFM (Figure 4c and d), LCNF-H72 was shown to contain shorter fibrils, likely due to its enhanced deconstruction resulting from the longer hydrolysis time. However, larger and incompletely hydrolyzed fibers could be observed with both the LCNF-H12 and LCNF-H72 substrates. The average thicknesses of the LCNF-H12 and LCNF-H72 fibers were calculated as 5.3 and 5.0 nm, respectively (Figure S3). White spherical lignin nanoparticles were observed in both samples, greater amounts were present in the LCNF-H72 sample, which was consistent with its higher lignin content.

Chemical and Crystalline Structures of LCNFs. The FTIR spectra of the sulfonated BCTMP (S-BCTMP), enzymatic hydrolyzed pulp (S-BCTMP-H12 and S-BCTMP-H72), and LCNFs (LCNF-H12 and LCNF-H72) indicated a relatively unchanged cellulose structure. For example, absorbance peaks at around 3340 (O−H stretching vibration), 2895 (C−H stretching), 1455 ($-CH_2$ symmetric bending vibration), 1370 (C−H bending vibration), 1159 (C−O−C stretching vibration), 1056 (C−O−C ring-stretching vibration), and 897 cm^{-1} (C−H deformation vibrations) all indicated no substantial changes,[51,52,57] while the characteristic lignin peaks at 1596, 1508 (C═C stretching of the aromatic skeletal), and 1265 cm^{-1} (C−O aryl group of lignin) (Figure 5a) confirmed that lignin was present after neutral sulphonation, enzymatic treatment, and mechanical treatment.[7,15]

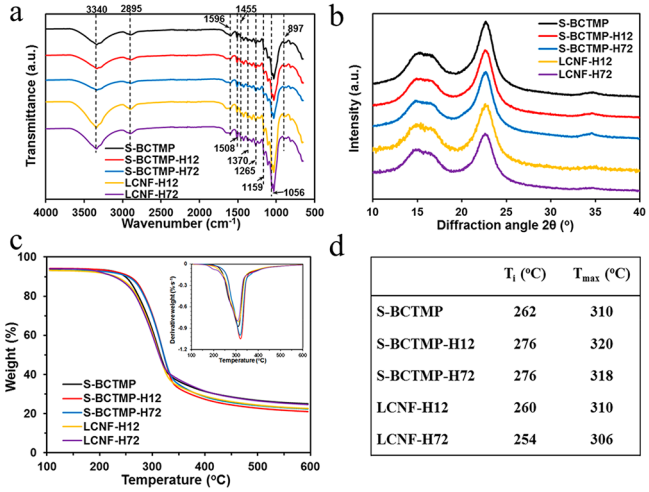

Figure 5. (a) ATR-FTIR spectra; (b) XRD spectra; (c) TGA curves with embedded DTGA curves; (d) table of degradation temperature for S-BCTMP, hydrolyzed S-BCTMP, and LCNFs.

When X-ray diffraction (XRD) was used to assess any crystallinity changes, the LCNFs showed the same pattern as the S-BCTMP and enzymatic hydrolyzed pulp (Figure 5b). The crystallinity index (CrI) is commonly determined from the height ratio between the intensity of the crystalline peak and the total intensity. However, it is generally acknowledged that the values derived via the peak height method tend to be higher while the peak deconvolution method, which considers the contributions from both the amorphous and crystalline cellulose, gives a more accurate crystallinity value.[37] The crystallinity of the S-BCTMP-H12 substrate (62%) was higher than that of the S-BCTMP (56%) substrate, likely because of hemicellulose removal and because the less-organized cellulose tends to get hydrolyzed faster than crystalline cellulose.[48−50]

Thermal Stability of LCNFs. Thermogravimetric analysis (TGA) was conducted next to compare the differences in thermal stability of S-BCTMP, enzymatic hydrolyzed pulp, and LCNFs samples. Previous work had shown that the thermal stability is influenced by the chemical composition, crystallinity, and surface area of the pulps.[58] The weight loss versus temperature (dW/dT) is summarized in Figure 5c, and the initial decomposing temperatures (T_i) and maximum degradation temperatures T_{max} are in Figure 5d. After hydrolysis, the

https://dx.doi.org/10.1021/acssuschemeng.0c05183
ACS Sustainable Chem. Eng. 2020, 8, 14955−14963

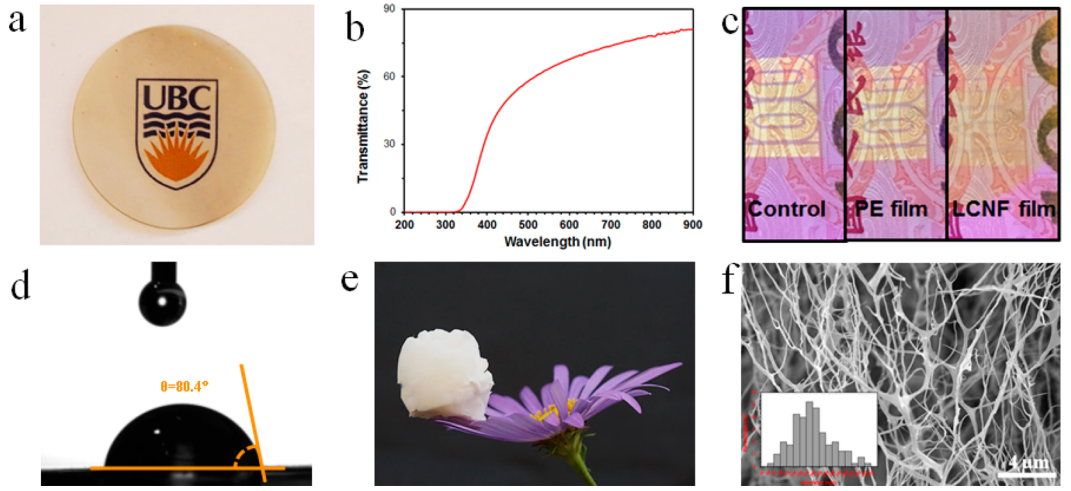

Figure 6. Characterization of the assembled structure from LCNF-H12. (a) Photos of film made from LCNF-H12; (b) UV−vis transmittance spectrum of the LCNF-H12 film; (c) photos demonstrating the UV-blocking performance of the LCNF-H12 film as compared to polyethylene (PE) film; (d) contact angle of the LCNF-H12 film; (e) white freeze-dried LCNF-H12 aerogel standing on the top of a flower; (f) SEM image of the freeze-dried LCNF-H12 aerogel, embedded with a width distribution of the submicron fibers.

consequential increase in cellulose crystallinity and lignin content resulted in an increase in the T_i and T_{max} values (Figure 5b and Table 1). It was apparent that nanofibrillation resulted in an increase in the surface area of the fibrils, resulting in reduced T_i and T_{max} of LCNFs when compared to the original feedstocks (Figure 5c). The T_{max} values of LCNF-H12 and LCNF-H72 were 310 and 306 °C, respectively, agreeing with the values of similar LCNF materials derived from hardwoods.[30] Because lignin is more thermally stable than cellulose and hemicellulose, the higher lignin-containing LCNF-H72 had a higher char residue than did the LCNF-H12.

Potential Applications of LCNFs. As greater amounts of the LCNF-H12 could be produced, the longer, more flexible nanofibrils present in this substrate were formed into an ultrathin (38.4 μm thick) film via vacuum filtration using a 0.2 μm filter membrane (Figure 6a). The observed brownish color was significantly darker than the translucent light white color of the LCNF-H12 aqueous suspension (Figure 3c), likely due to the accumulation of the lignin within the solid film. Although the UV−vis transmittance spectrum indicated blockage of UV light from 200 to 325 nm, a high transmittance to visible light was apparent, reaching 78% transmittance at 800 nm (Figure 6b). The UV-blocking performance of the LCNF film was further demonstrated by illumination via a UV flashlight. At a 50 cm distance, the "100" UV pattern could be clearly illuminated when there is no substrate or a PE substrate between the flashlight and the UV pattern (Figure 6c). However, when the LCNF film was placed between the flashlight and the UV pattern, the UV pattern became much fainter, further confirming the UV-blocking performance of the LCNF film. This was likely due to lignin-associated UV-absorbing functional groups, such as phenolics, ketones, and other chromophores, acting as natural broad-spectrum UV blockers.[59] When the hydrophobic nature of the LCNF was assessed using the water contact angle assay, although it was reduced from 82.8° to 80.4° (Figure 6d) after 2 min, it was significantly higher than those of CNFs derived from holocellulose (normally between 30° and 40°).[15,20] This lignin-induced hydrophobicity suggested that the LCNFs could have good compatibility with other hydrophobic polymers when used as nanofillers.

Further work indicated that ultralightweight aerogels could also be fabricated from the LCNF-H12 substrate (Figure 6e) because freeze-drying an aqueous suspension at 0.1 wt % resulted in a fluffy, foam-like material that could potentially be applied to ultraporous types of materials.[60] The aerogel was composed of ultrafine, submicron fibers of a 50−370 nm diameter (179.9 nm in average) and larger film- or ribbon-like structures (Figure 6f), similar to those previously observed in mechanically defibrillated cellulose nanofibrils.[61,62]

CONCLUSIONS

It was apparent that sulphonation of BCTM pulps could enhance both cellulose hydrolysis and the production of lignin-containing cellulose nanofibrils (LCNFs). A 12 h hydrolysis seemed to be optimum for both sugars and LCNFs production with enzyme treatment, followed by treatment in a blender and ultrasonicator, enhancing the delamination and defibrillation of the residual fibers. The LCNFs were relatively homogeneous, had a relatively high lignin content, and were well-dispersed in water. Films made from the LCNFs showed a high contact angle and had a high transmittance to visible light and strong UV-blocking properties. The LCNFs could also be used to make ultralightweight aerogels with potential applications as ultraporous types of materials.

ASSOCIATED CONTENT

Supporting Information

The Supporting Information is available free of charge at https://pubs.acs.org/doi/10.1021/acssuschemeng.0c05183.

Chemical composition of the hydrolyzed S-BCTMP and the prepared LCNFs; TEM images of LCNFs prepared by blending and ultrasonication; and width and height distribution of LCNFs (PDF)

AUTHOR INFORMATION

Corresponding Authors

Feng Jiang − *Sustainable Functional Biomaterials Lab, Department of Wood Science, University of British Columbia, Vancouver, British Columbia V6T 1Z4, Canada;* orcid.org/0000-0003-2497-9922; Email: feng.jiang@ubc.ca

https://dx.doi.org/10.1021/acssuschemeng.0c05183
ACS Sustainable Chem. Eng. 2020, 8, 14955−14963

Jack N. Saddler − *Forest Products Biotechnology/Bioenergy Group, Department of Wood Science, University of British Columbia, Vancouver, British Columbia V6T 1Z4, Canada;* orcid.org/0000-0002-8689-3967; Email: jack.saddler@ubc.ca

Authors

Xushen Han − *National Engineering Research Center for Integrated Utilization of Salt Lake Resources and State Key Laboratory of Bioreactor Engineering, East China University of Science and Technology, Shanghai 200237, P. R. China; Forest Products Biotechnology/Bioenergy Group, Department of Wood Science, University of British Columbia, Vancouver, British Columbia V6T 1Z4, Canada;* orcid.org/0000-0002-0436-478X

Ran Bi − *Forest Products Biotechnology/Bioenergy Group, Department of Wood Science, University of British Columbia, Vancouver, British Columbia V6T 1Z4, Canada*

Hale Oguzlu − *Sustainable Functional Biomaterials Lab, Department of Wood Science, University of British Columbia, Vancouver, British Columbia V6T 1Z4, Canada*

Masatsugu Takada − *Forest Products Biotechnology/Bioenergy Group, Department of Wood Science, University of British Columbia, Vancouver, British Columbia V6T 1Z4, Canada*

Jungang Jiang − *Sustainable Functional Biomaterials Lab, Department of Wood Science, University of British Columbia, Vancouver, British Columbia V6T 1Z4, Canada;* orcid.org/0000-0002-6761-9647

Jie Bao − *State Key Laboratory of Bioreactor Engineering, East China University of Science and Technology, Shanghai 200237, P. R. China;* orcid.org/0000-0001-6521-3099

Complete contact information is available at: https://pubs.acs.org/10.1021/acssuschemeng.0c05183

Notes

The authors declare no competing financial interest.

■ ACKNOWLEDGMENTS

We thank NSERC for financial support and the China Scholarship Council (CSC) for supporting X.H. (CSC no. 201806740032). We also thank colleagues in Wood Science and the Forest Products Biotechnology/Bioenergy group, especially Yuhang Ye, Jie Wu, Kevin Aissa, Rou Yi Yeap, Drake Mboowa, Fredrik Nielsen, and Yaseen Mottiar, for their help and support.

■ REFERENCES

(1) Klemm, D.; Kramer, F.; Moritz, S.; Lindström, T.; Ankerfors, M.; Gray, D.; Dorris, A. Nanocelluloses: A New Family of Nature-Based Materials. *Angew. Chem., Int. Ed.* **2011**, *50* (24), 5438−5466.

(2) Lin, N.; Dufresne, A. Nanocellulose in Biomedicine: Current Status and Future Prospect. *Eur. Polym. J.* **2014**, *59*, 302−325.

(3) Zheng, Q.; Cai, Z.; Ma, Z.; Gong, S. Cellulose Nanofibril/Reduced Graphene Oxide/Carbon Nanotube Hybrid Aerogels for Highly Flexible and All-Solid-State Supercapacitors. *ACS Appl. Mater. Interfaces* **2015**, *7* (5), 3263−3271.

(4) Han, X.; Ye, Y.; Lam, F.; Pu, J.; Jiang, F. Hydrogen-Bonding-Induced Assembly of Aligned Cellulose Nanofibers into Ultrastrong and Tough Bulk Materials. *J. Mater. Chem. A* **2019**, *7* (47), 27023−27031.

(5) Nechyporchuk, O.; Belgacem, M. N.; Bras, J. Production of Cellulose Nanofibrils: A Review of Recent Advances. *Ind. Crops Prod.* **2016**, *93*, 2−25.

(6) Bian, H.; Chen, L.; Dai, H.; Zhu, J. Y. Effect of Fiber Drying on Properties of Lignin Containing Cellulose Nanocrystals and Nanofibrils Produced through Maleic Acid Hydrolysis. *Cellulose* **2017**, *24* (10), 4205−4216.

(7) Bian, H.; Chen, L.; Dai, H.; Zhu, J. Y. Integrated Production of Lignin Containing Cellulose Nanocrystals (LCNC) and Nanofibrils (LCNF) Using an Easily Recyclable Di-Carboxylic Acid. *Carbohydr. Polym.* **2017**, *167*, 167−176.

(8) Patankar, S. C.; Renneckar, S. Greener Synthesis of Nanofibrillated Cellulose Using Magnetically Separable TEMPO Nanocatalyst. *Green Chem.* **2017**, *19* (20), 4792−4797.

(9) Long, L.; Tian, D.; Hu, J.; Wang, F.; Saddler, J. A Xylanase-Aided Enzymatic Pretreatment Facilitates Cellulose Nanofibrillation. *Bioresour. Technol.* **2017**, *243*, 898−904.

(10) Pääkko, M.; Ankerfors, M.; Kosonen, H.; Nykänen, A.; Ahola, S.; Österberg, M.; Ruokolainen, J.; Laine, J.; Larsson, P. T.; Ikkala, O.; Lindström, T. Enzymatic Hydrolysis Combined with Mechanical Shearing and High-Pressure Homogenization for Nanoscale Cellulose Fibrils and Strong Gels. *Biomacromolecules* **2007**, *8* (6), 1934−1941.

(11) Zhu, J. Y.; Sabo, R.; Luo, X. Integrated Production of Nano-Fibrillated Cellulose and Cellulosic Biofuel (Ethanol) by Enzymatic Fractionation of Wood Fibers. *Green Chem.* **2011**, *13* (5), 1339−1344.

(12) Abe, K.; Nakatsubo, F.; Yano, H. High-Strength Nanocomposite Based on Fibrillated Chemi-Thermomechanical Pulp. *Compos. Sci. Technol.* **2009**, *69* (14), 2434−2437.

(13) Ewulonu, C. M.; Liu, X.; Wu, M.; Yong, H. Lignin-Containing Cellulose Nanomaterials: A Promising New Nanomaterial for Numerous Applications. *J. Bioresour. Bioprod.* **2019**, *4* (1), 3−10.

(14) Osong, S. H.; Norgren, S.; Engstrand, P. An Approach to Produce Nano-Ligno-Cellulose from Mechanical Pulp Fine Materials. *Nord. Pulp Pap. Res. J.* **2013**, *28* (4), 472−479.

(15) Wen, Y.; Yuan, Z.; Liu, X.; Qu, J.; Yang, S.; Wang, A.; Wang, C.; Wei, B.; Xu, J.; Ni, Y. Preparation and Characterization of Lignin-Containing Cellulose Nanofibril from Poplar High-Yield Pulp via TEMPO-Mediated Oxidation and Homogenization. *ACS Sustainable Chem. Eng.* **2019**, *7* (6), 6131−6139.

(16) Bajpai, P. *Environmentally Friendly Production of Pulp and Paper*; John Wiley & Sons, Inc.: Hoboken, NJ, 2010; DOI: 10.1002/9780470649657.ch1.

(17) Sixta, H. *Handbook of Pulp*; Wiley-VCH Verlag GmbH & Co. KGaH: Weinheim, Germany, 2006; DOI: 10.1002/9783527619887.

(18) Takada, M.; Chandra, R.; Wu, J.; Saddler, J. N. The Influence of Lignin on the Effectiveness of Using a Chemithermomechanical Pulping Based Process to Pretreat Softwood Chips and Pellets Prior to Enzymatic Hydrolysis. *Bioresour. Technol.* **2020**, *302*, 122895.

(19) Arola, S.; Malho, J. M.; Laaksonen, P.; Lille, M.; Linder, M. B. The Role of Hemicellulose in Nanofibrillated Cellulose Networks. *Soft Matter* **2013**, *9* (4), 1319−1326.

(20) Chen, Y.; Fan, D.; Han, Y.; Lyu, S.; Lu, Y.; Li, G.; Jiang, F.; Wang, S. Effect of High Residual Lignin on the Properties of Cellulose Nanofibrils/Films. *Cellulose* **2018**, *25* (11), 6421−6431.

(21) Habibi, Y. Key Advances in the Chemical Modification of Nanocelluloses. *Chem. Soc. Rev.* **2014**, *43* (5), 1519−1542.

(22) Jiang, F.; Hsieh, Y. Lo. Holocellulose Nanocrystals: Amphiphilicity, Oil/Water Emulsion, and Self-Assembly. *Biomacromolecules* **2015**, *16* (4), 1433−1441.

(23) Nair, S. S.; Yan, N. Effect of High Residual Lignin on the Thermal Stability of Nanofibrils and Its Enhanced Mechanical Performance in Aqueous Environments. *Cellulose* **2015**, *22* (5), 3137−3150.

(24) Nair, S. S.; Kuo, P. Y.; Chen, H.; Yan, N. Investigating the Effect of Lignin on the Mechanical, Thermal, and Barrier Properties of Cellulose Nanofibril Reinforced Epoxy Composite. *Ind. Crops Prod.* **2017**, *100*, 208−217.

(25) Tarrés, Q.; Ehman, N. V.; Vallejos, M. E.; Area, M. C.; Delgado-Aguilar, M.; Mutjé, P. Lignocellulosic Nanofibers from Triticale Straw: The Influence of Hemicelluloses and Lignin in Their Production and Properties. *Carbohydr. Polym.* **2017**, *163*, 20−27.

(26) Rojo, E.; Peresin, M. S.; Sampson, W. W.; Hoeger, I. C.; Vartiainen, J.; Laine, J.; Rojas, O. J. Comprehensive Elucidation of the Effect of Residual Lignin on the Physical, Barrier, Mechanical and Surface Properties of Nanocellulose Films. *Green Chem.* **2015**, *17* (3), 1853−1866.
(27) Spence, K. L.; Venditti, R. A.; Habibi, Y.; Rojas, O. J.; Pawlak, J. J. The Effect of Chemical Composition on Microfibrillar Cellulose Films from Wood Pulps: Mechanical Processing and Physical Properties. *Bioresour. Technol.* **2010**, *101* (15), 5961−5968.
(28) Iwamoto, S.; Abe, K.; Yano, H. The Effect of Hemicelluloses on Wood Pulp Nanofibrillation and Nanofiber Network Characteristics. *Biomacromolecules* **2008**, *9* (3), 1022−1026.
(29) Diop, C. I. K.; Tajvidi, M.; Bilodeau, M. A.; Bousfield, D. W.; Hunt, J. F. Evaluation of the Incorporation of Lignocellulose Nanofibrils as Sustainable Adhesive Replacement in Medium Density Fiberboards. *Ind. Crops Prod.* **2017**, *109* (July), 27−36.
(30) Herrera, M.; Thitiwutthisakul, K.; Yang, X.; Rujitanaroj, P. on; Rojas, R.; Berglund, L. Preparation and Evaluation of High-Lignin Content Cellulose Nanofibrils from Eucalyptus Pulp. *Cellulose* **2018**, *25* (5), 3121−3133.
(31) Chandra, R. P.; Chu, Q. L.; Hu, J.; Zhong, N.; Lin, M.; Lee, J. S.; Saddler, J. The Influence of Lignin on Steam Pretreatment and Mechanical Pulping of Poplar to Achieve High Sugar Recovery and Ease of Enzymatic Hydrolysis. *Bioresour. Technol.* **2016**, *199*, 135−141.
(32) Jiang, J.; Carrillo-Enríquez, N. C.; Oguzlu, H.; Han, X.; Bi, R.; Song, M.; Saddler, J. N.; Sun, R.-C.; Jiang, F. High Production Yield and More Thermally Stable Lignin-Containing Cellulose Nanocrystals Isolated Using a Ternary Acidic Deep Eutectic Solvent. *ACS Sustainable Chem. Eng.* **2020**, *8* (18), 7182−7191.
(33) Jiang, J.; Carrillo-Enríquez, N. C.; Oguzlu, H.; Han, X.; Bi, R.; Saddler, J. N.; Sun, R. C.; Jiang, F. Acidic Deep Eutectic Solvent Assisted Isolation of Lignin Containing Nanocellulose from Thermomechanical Pulp. *Carbohydr. Polym.* **2020**, *247* (July), 116727.
(34) Chandra, R. P.; Wu, J.; Saddler, J. N. The Application of Fiber Quality Analysis (FQA) and Cellulose Accessibility Measurements to Better Elucidate the Impact of Fiber Curls and Kinks on the Enzymatic Hydrolysis of Fibers. *ACS Sustainable Chem. Eng.* **2019**, *7* (9), 8827−8833.
(35) Chandra, R. P.; Saddler, J. N. Use of the Simons' Staining Technique to Assess Cellulose Accessibility in Pretreated Substrates. *Ind. Biotechnol.* **2012**, *8* (4), 230−237.
(36) Katz, S.; Beatson, R. P.; Scallan, A. M. The Determination of Strong and Weak Acidic Groups in Sulfite Pulps. *Sven. Papperstidn.* **1984**, *87*, 48−53.
(37) Park, S.; Baker, J. O.; Himmel, M. E.; Parilla, P. A.; Johnson, D. K. Cellulose Crystallinity Index: Measurement Techniques and Their Impact on Interpreting Cellulase Performance. *Biotechnol. Biofuels* **2010**, *3*, 10.
(38) Scherrer, P. Estimation of the Size and Internal Structure of Colloidal Particles by Means of Röntgen Rays. *Nachr. Ges. Wiss. Göttingen* **1918**, *2*, 98−100.
(39) Kumar, L.; Arantes, V.; Chandra, R.; Saddler, J. The Lignin Present in Steam Pretreated Softwood Binds Enzymes and Limits Cellulose Accessibility. *Bioresour. Technol.* **2012**, *103* (1), 201−208.
(40) Chandra, R. P.; Bura, R.; Mabee, W. E.; Berlin, A.; Pan, X.; Saddler, J. N. Substrate Pretreatment: The Key to Effective Enzymatic Hydrolysis of Lignocellulosics? In *Biofuels*; Springer: Berlin/Heidelberg, 2007; pp 67−93; DOI: 10.1007/10_2007_064.
(41) van der Zwan, T.; Chandra, R. P.; Saddler, J. N. Laccase-Mediated Hydrophilization of Lignin Decreases Unproductive Enzyme Binding but Limits Subsequent Enzymatic Hydrolysis at High Substrate Concentrations. *Bioresour. Technol.* **2019**, *292*, 121999.
(42) Beyene, D.; Chae, M.; Dai, J.; Danumah, C.; Tosto, F.; Demesa, A. G.; Bressler, D. C. Enzymatically-Mediated Co-Production of Cellulose Nanocrystals and Fermentable Sugars. *Catalysts* **2017**, *7* (11), 322.
(43) Wyman, C. E.; Dale, B. E. Producing Biofuels via the Sugar Platform. *Chem. Eng. Prog.* **2015**, *111* (3), 45−57.
(44) Han, X.; Bao, J. General Method to Correct the Fluctuation of Acid Based Pretreatment Efficiency of Lignocellulose for Highly Efficient Bioconversion. *ACS Sustainable Chem. Eng.* **2018**, *6* (3), 4212−4219.
(45) Han, X.; Hong, F.; Liu, G.; Bao, J. An Approach of Utilizing Water-Soluble Carbohydrates in Lignocellulose Feedstock for Promotion of Cellulosic l -Lactic Acid Production. *J. Agric. Food Chem.* **2018**, *66* (39), 10225−10232.
(46) Han, X.; Li, L.; Wei, C.; Zhang, J.; Bao, J. Facilitation of L-Lactic Acid Fermentation by Lignocellulose Biomass Rich in Vitamin B Compounds. *J. Agric. Food Chem.* **2019**, *67* (25), 7082−7086.
(47) Han, X.; Li, L.; Bao, J. Microbial Extraction of Biotin from Lignocellulose Biomass and Its Application on Glutamic Acid Production. *Bioresour. Technol.* **2019**, *288*, 121523.
(48) Gourlay, K.; Hu, J.; Arantes, V.; Penttilä, M.; Saddler, J. N. The Use of Carbohydrate Binding Modules (CBMs) to Monitor Changes in Fragmentation and Cellulose Fiber Surface Morphology during Cellulase- And Swollenin-Induced Deconstruction of Lignocellulosic Substrates. *J. Biol. Chem.* **2015**, *290* (5), 2938−2945.
(49) Hidayat, B. J.; Felby, C.; Johansen, K. S.; Thygesen, L. G. Cellulose Is Not Just Cellulose: A Review of Dislocations as Reactive Sites in the Enzymatic Hydrolysis of Cellulose Microfibrils. *Cellulose* **2012**, *19* (5), 1481−1493.
(50) Lynd, L. R.; Weimer, P. J.; van Zyl, W. H.; Pretorius, I. S. Microbial Cellulose Utilization: Fundamentals and Biotechnology. *Microbiol. Mol. Biol. Rev.* **2002**, *66* (3), 506−577.
(51) Jiang, F.; Han, S.; Hsieh, Y. Lo. Controlled Defibrillation of Rice Straw Cellulose and Self-Assembly of Cellulose Nanofibrils into Highly Crystalline Fibrous Materials. *RSC Adv.* **2013**, *3* (30), 12366−12375.
(52) Jiang, F.; Hsieh, Y. Lo. Chemically and Mechanically Isolated Nanocellulose and Their Self-Assembled Structures. *Carbohydr. Polym.* **2013**, *95* (1), 32−40.
(53) Isogai, A.; Saito, T.; Fukuzumi, H. TEMPO-Oxidized Cellulose Nanofibers. *Nanoscale* **2011**, *3* (1), 71−85.
(54) Bentivenga, G.; Bonini, C.; D'Auria, M.; De Bona, A.; Mauriello, G. Singlet Oxygen Mediated Degradation of Klason Lignin. *Chemosphere* **1999**, *39* (14), 2409−2417.
(55) Kline, L. M.; Hayes, D. G.; Womac, A. R.; Labbe, N. Simplified Determination of Lignin Content in Hard and Soft Woods via UV-Spectrophotometric Analysis of Biomass Dissolved in Ionic Liquids. *BioResources* **2010**, *5* (3), 1366−1383.
(56) Sun, R.; Tomkinson, J.; Mao, F. C.; Sun, X. F. Physicochemical Characterization of Lignins from Rice Straw by Hydrogen Peroxide Treatment. *J. Appl. Polym. Sci.* **2001**, *79* (4), 719−732.
(57) Luo, J.; Huang, K.; Xu, Y.; Fan, Y. A Comparative Study of Lignocellulosic Nanofibrils Isolated from Celery Using Oxalic Acid Hydrolysis Followed by Sonication and Mechanical Fibrillation. *Cellulose* **2019**, *26* (9), 5237−5246.
(58) Raveendran, K.; Ganesh, A.; Khilar, K. C. Pyrolysis Characteristics of Biomass and Biomass Components. *Fuel* **1996**, *75* (8), 987−998.
(59) Sadeghifar, H.; Venditti, R.; Jur, J.; Gorga, R. E.; Pawlak, J. J. Cellulose-Lignin Biodegradable and Flexible UV Protection Film. *ACS Sustainable Chem. Eng.* **2017**, *5* (1), 625−631.
(60) Chen, Y.; Fan, D.; Lyu, S.; Li, G.; Jiang, F.; Wang, S. Elasticity-Enhanced and Aligned Structure Nanocellulose Foam-like Aerogel Assembled with Cooperation of Chemical Art and Gradient Freezing. *ACS Sustainable Chem. Eng.* **2019**, *7* (1), 1381−1388.
(61) Jiang, F.; Hsieh, Y. Lo. Assembling and Redispersibility of Rice Straw Nanocellulose: Effect of Tert-Butanol. *ACS Appl. Mater. Interfaces* **2014**, *6* (22), 20075−20084.
(62) Jiang, F.; Kondo, T.; Hsieh, Y. Lo. Rice Straw Cellulose Nanofibrils via Aqueous Counter Collision and Differential Centrifugation and Their Self-Assembled Structures. *ACS Sustainable Chem. Eng.* **2016**, *4* (3), 1697−1706.

https://dx.doi.org/10.1021/acssuschemeng.0c05183
ACS Sustainable Chem. Eng. 2020, 8, 14955−14963